THE JOURNAL OF BIOLOGICAL CHEMISTRY Vol. 279, No. 12, Issue of March 19, pp. 11392–11401, 2004
Printed in U.S.A.

Peroxisome Proliferator-activated Receptor γ Induces a Phenotypic Switch from Activated to Quiescent Hepatic Stellate Cells*

Received for publication, September 16, 2003, and in revised form, December 24, 2003
Published, JBC Papers in Press, December 31, 2003, DOI 10.1074/jbc.M310284200

Saswati Hazra‡, Shigang Xiong‡, Jiaohong Wang‡, Richard A. Rippe§, V. Krishna K. Chatterjee¶, and Hidekazu Tsukamoto‡‖****

From the ‡Department of Pathology, Keck School of Medicine of the University of Southern California, Los Angeles, California 90033, the §Department of Medicine, University of North Carolina, Chapel Hill, North Carolina 27599-7032, the ¶Department of Medicine, University of Cambridge, Addenbrooke's Hospital, Cambridge CB2 2QQ, United Kingdom, and the ‖Department of Veterans Affairs Greater Los Angeles Healthcare System, Los Angeles, California 90073

Depletion of peroxisome proliferator-activated receptor γ (PPARγ) accompanies myofibroblastic transdifferentiation of hepatic stellate cells (HSC), the primary cellular event underlying liver fibrogenesis. The treatment of activated HSC *in vitro* or *in vivo* with synthetic PPARγ ligands suppresses the fibrogenic activity of HSC. However, it is uncertain whether PPARγ is indeed a molecular target of this effect, because the ligands are also known to have receptor-independent actions. To test this question, the present study examined the effects of forced expression of PPARγ via an adenoviral vector on morphologic and biochemical features of culture-activated HSC. The vector-mediated expression of PPARγ itself is sufficient to reverse the morphology of activated HSC to the quiescent phenotype with retracted cytoplasm, prominent dendritic processes, reduced stress fibers, and accumulation of retinyl palmitate. These effects are abrogated by concomitant expression of a dominant negative mutant of PPARγ that prevents transactivation of but not binding to the PPAR response element. PPARγ expression also inhibits the activation markers such as the expression of α-smooth muscle actin, type I collagen, and transforming growth factor β1; DNA synthesis; and JunD binding to the activator protein-1 (AP-1) site and AP-1 promoter activity. Inhibited JunD activity by PPARγ is not due to reduced JunD expression or JNK activity or to a competition for p300. But it is due to a JunD-PPARγ interaction as demonstrated by co-immunoprecipitation and glutathione *S*-transferase pull-down analysis. Further, the use of deletion constructs reveals that the DNA binding region of PPARγ is the JunD interaction domain. In summary, our results demonstrate that the restoration of PPARγ reverses the activated HSC to the quiescent phenotype and suppresses AP-1 activity via a physical interaction between PPARγ and JunD.

Hepatic stellate cells (HSC)[1] are vitamin A-storing pericytes in the subendothelial space of the liver. Upon injury to the liver, HSC become transdifferentiated into myofibroblastic cells to participate in wound healing (1). This transdifferentiation is characterized by reduced vitamin A content, increased cell proliferation and migration, enhanced matrix protein expression, and induced expression of α-smooth muscle actin (1). This response of HSC constitutes the normal, reparative homeostatic response of the liver to injury. However, dysregulation of HSC leads to excessive accumulation of extracellular matrices, resulting in liver fibrosis and cirrhosis. No curative medical treatments are available for cirrhosis except liver transplantation, and a precise understanding of transdifferentiation of HSC is the prerequisite for eventual identification of "dysregulation" and future developments of specific therapeutic modalities for the disease. To this end, much investigative effort has been made to characterize transcriptional regulation that underlies HSC transdifferentiation. Such examples include identification of Kruppel-like factor 6, a differentially expressed zinc finger protein in activated HSC *in vitro* and *in vivo* (2). This transcription factor binds to the GC box sites of TGFβ1, TGFβ receptor type I and II (2), urokinase-type plasminogen activator (3), and α1(I) procollagen (2) and induces transcription of these fibrogenic genes. The myofibroblastic phenotype seen in activated HSC is best characterized by induction of α-smooth muscle actin that is mediated by c-Myb binding to an E-box element in its promoter (4). The significance of this mode of regulation is supported by the demonstration of prevention of the myofibroblastic phenotypic switch by the treatment of HSC with antisense oligonucleotides for c-Myb (4). Sustained NF-κB activation confers activated HSC their proliferative and antiapoptotic status that may be important in progressive liver fibrogenesis (5). NF-κB may also mediate inflammatory responses by HSC via induction of chemokines and adhesion molecules (6, 7). Increased activator protein-1 (AP-1) activity is essential for induction of matrix metalloproteinase (8), tissue inhibitor of matrix metalloproteinase-1, and interleukin-6 (9) gene transcription in activated HSC, where JunD is shown to play a pivotal role (9).

* This study was supported by National Institutes of Health Grants R37AA06603, P50AA11999 (to the USC-UCLA Research Center for Alcoholic Liver and Pancreatic Diseases), P30DK48522 (to the USC Research Center for Liver Diseases), and R24AA12885 (to the Non-Parenchymal Liver Cell Core) and by the Medical Research Service of the Department of Veterans Affairs. The work presented in this article is in partial fulfillment of Ph.D. requirements at the University of Southern California (for S. H.). The costs of publication of this article were defrayed in part by the payment of page charges. This article must therefore be hereby marked "*advertisement*" in accordance with 18 U.S.C. Section 1734 solely to indicate this fact.

** To whom correspondence should be addressed: Keck School of Medicine of the University of Southern California, 1333 San Pablo St., MMR-402, Los Angeles, CA 90089-9141. Tel.: 323-442-5107; Fax: 323-442-3126; E-mail: htsukamo@usc.edu.

[1] The abbreviations used are: HSC, hepatic stellate cell(s); PPARγ, peroxisome proliferator-activated receptor γ; PPRE, peroxisome proliferator-activated receptor response element; AP, activator protein, TGFβ and TGFβ1, transforming growth factor β and β1, respectively; RXRα, retinoid X receptor α; JNK, c-Jun N-terminal kinase; GST, glutathione *S*-transferase; MOI, multiplicity of infection; DMEM, Dulbecco's modified Eagle's medium; FBS, fetal bovine serum; GFP, green fluorescent protein; CREB, cAMP-response element-binding protein; CBP, CREB-binding protein; HPLC, high pressure liquid chromatography.

A complexity in the understanding of HSC differentiation is underscored by different cellular phenotypes that HSC are shown to express. In addition to the myofibroblastic phenotype exhibited by activated HSC, they also express MyoD, the myogenic transcription factor specific for skeletal muscle (9). Neuronal markers such as GFAP (10), N-CAM (6), nestin (11), and synaptophysin (12) are also expressed in HSC, suggesting the neural phenotype and that N-CAM and nestin are induced in activated HSC. Activated HSC express leptin (13), an adipocyte-specific gene, raising an intriguing possibility that HSC may also share the adipocytic phenotype. In fact, the quiescent HSC is laden with lipids including triglycerides, cholesterol, and phospholipids in addition to retinyl esters (14). In support of this notion, peroxisome proliferator-activated receptor γ (PPARγ), one of the key transcription factors for adipocyte differentiation (15), is expressed in the quiescent HSC (16–18), and its expression and activity decrease in HSC activation *in vitro* (16, 17) and *in vivo* (16). Further, the treatment of culture-activated HSC with the natural or synthetic ligands for PPARγ suppresses many functional parameters of the cell activation, including cell proliferation (17), expression of collagen, TGFβ, α-smooth muscle actin, monocyte chemotactic protein-1 genes, and chemotaxis (16, 18). More importantly, the treatment of the animal models of liver fibrosis with the PPARγ ligands ameliorates not only induction of fibrosis but also progression of preexisting fibrosis (17). Thus, these findings support the hypothesis that the maintenance of the quiescent state of HSC requires PPARγ and depletion of this adipogenic transcription factor underlies activation of HSC that can be circumvented by the ligand treatment. However, the ligands for PPARγ are also known to have receptor-independent effects. Using the embryonic stem cells from PPARγ null mice, neither macrophage differentiation nor anti-inflammatory effects of synthetic PPARγ ligands are shown to be dependent on PPARγ (19). Indeed, the PPARγ ligand 15-deoxyprostaglandin J_2 suppresses NF-κB activation by directly inhibiting IκB kinase in a PPARγ-independent manner (20). Troglitazone also selectively induces early growth response-1 gene independently of PPARγ (21). Mitogen-activated protein kinases such as c-Jun N-terminal kinase (JNK), p38, and extracellular signal-regulated kinase are activated by PPARγ ligands such as 15-deoxyprostaglandin J_2 and ciglitazone in astrocytes and preadipocytes through the mechanisms that are independent of PPARγ but involving reactive oxygen species (22). Therefore, it is yet to be determined whether PPARγ directly inhibits HSC activation. In order to test this question, the present study was undertaken to express PPARγ via an adenoviral vector in culture-activated HSC and to determine its effects on the cell activation. Our results demonstrate that the restoration of PPARγ in activated HSC induces a reversal of the morphological features of HSC to the quiescent phenotype associated with inhibition of the known activation markers such as induced α-smooth muscle actin, collagen, and TGFβ expression; enhanced DNA synthesis; increased AP-1 binding; and promoter activity. Inhibition of AP-1 binding is due to PPARγ-mediated interference of JunD binding but not to suppression of JunD expression or JNK activity. Further, our results demonstrate a direct interaction of the PPARγ DNA binding domain with JunD that appears to underlie inhibited JunD binding to the AP-1 site.

MATERIALS AND METHODS

HSC Isolation and Culture—HSC were isolated from normal male Wister rats as previously described (23) by the Non-Parenchymal Liver Cell Core of the USC-UCLA Research Center for Alcoholic Liver and Pancreatic Diseases. The use of animals for this study was approved by the Institutional Animal Care and Use Committee of the University of Southern California (protocol 9823). In brief, the liver was sequentially digested with Pronase and type IV collagenase to isolate nonparenchymal cells. These cells were subsequently subjected to arabinogalactan gradient ultracentrifugation to collect a pure fraction of HSC from the interface between the medium and a density of 1.035. The purity of isolated HSC was examined by phase-contrast microscopy, UV-excited fluorescence microscopy, and the viability by trypan blue exclusion. Isolated HSC from normal rats were cultured in a 100-mm plastic dish, 6- or 12-well plates with low glucose DMEM supplemented with 10% fetal bovine serum (FBS), 100 mg/ml streptomycin, 10,000 units/ml penicillin, and 25 μg/ml amphotericin B. The cultures were maintained for 7 days before the addition of viral vectors. In addition, a spontaneously immortalized HSC line established from experimental biliary liver fibrosis (24) was maintained in culture in 6-well plates with low glucose DMEM supplemented with 10% FBS and used for a transient transfection experiment for AP-1 promoter activity.

Construction of Viral Vectors and Transduction of the Viral Vector-mediated Genes—Full-length PPARγ1 cDNA was cloned from pCMX-PPARγ into the transfer vector, subsequently allowing homologous recombination with the pAdEasy-1 adenoviral plasmid containing GFP (Stratagene, La Jolla, CA). GFP alone was used as a control for PPARγ (Ad.GFP). An adenoviral vector expressing a dominant negative mutant form of PPARγ with a GFP tag (Ad.dn.PPARγ) was used. This dn.PPARγ carries the mutations at leucine and glutamic acid residues in the conserved AF-2 region of the C-terminal end. These mutations cause inhibition of recruitment of coactivators such as CBP and SRC-1 and ligand-dependent release of corepressors while promoting the basal recruitment of corepressors (25). All adenoviral vectors (Ad.GFP, Ad.PPARγ, and Ad.dn.PPARγ) were propagated using 293A cells in high glucose DMEM medium containing 5% FBS and then purified using cesium chloride gradient followed by dialysis for removing cesium chloride. The viral particle was titrated by the $TCID_{50}$ (tissue culture infectious dose 50) method. Briefly, dilutions of viruses were incubated with 293-A cells in 96-well plates, and the presence or absence of cytopathic effect in each well was determined for titration. A multiplicity of infection (MOI) of 100 was used for the efficient tansduction of viral vector-mediated genes in activated HSC without any toxicity. HSC were cultured for 7 days. On day 7 of culture, cells were transduced with Ad.GFP, Ad.PPARγ, or Ad.dn.PPARγ or in combination using a total MOI of 100. The next day, medium was changed and cultured for another 4 days.

DNA Synthesis—DNA synthesis was determined by the rate of [^{3}H]thymidine incorporation into DNA. Activated HSC were cultured in 24-well plates (27,000 cells/well) and were transduced with Ad.GFP or Ad.PPARγ and cultured for an additional 5 days. On the 4th day after infection, [*methyl*-^{3}H]thymidine (PerkinElmer Life Sciences) (1 μCi/ml) was added into each well and incubated overnight. After washing the cells, DNA was precipitated with 10% trichloroacetic acid at 4 °C. After several washes of the trichloroacetic acid precipitates, incorporation of [^{3}H]thymidine into DNA was determined by counting the radioactivity of the precipitates using liquid scintillation counter. The count was standardized by the cell number.

RNA Extraction and Real Time PCR—Total RNA was extracted from HSC transduced with Ad.GFP, Ad.PPAR plus Ad.GFP, or Ad.PPARγ plus Ad.dn.PPARγ using Trizol reagent (Invitrogen). Two micrograms of RNA were reverse-transcribed at 37 °C for 60 min with Moloney murine leukemia virus reverse transcriptase. For PCR analysis, the synthesized cDNA was amplified using primers for PPARγ, α1(I) procollagen, TGFβ1, and β-actin (16). For real time PCR, 2 ng of total RNA was used in a 20-μl reaction for reverse transcription for 50 min followed by 40 cycles of PCR to produce PCR products using the TaqMan Gold RT-PCR kit (Applied Biosystems, Foster city, CA). Probes were 5,6 carboxyl fluorescein amidite labeled at the 5′-end and black hole quencher-1 labeled at the 3′-end (Biosearch Technologies Inc., Novato, CA). Here, ABI 7700 SDS was used as a detection system. Each C_t value was first normalized to the respective glyceraldehyde-3-phosphate dehydrogenase C_t value of a sample and subsequently to a control sample. A difference in -fold was calculated from these C_t values.

Electrophoretic Mobility Gel Shift Assay—HSC nuclear proteins (5–10 μg) or PPARγ, JunD, or RXRα *in vitro* translated using the coupled transcription/translation systems (Promega, Madison, WI) were incubated in a reaction mixture (20 mM HEPES, pH 7.6, 100 mM KCl, 0.2 mM EDTA, 2 mM dithiothreitol, 20% glycerol, 200 μg/ml poly(dI-dC)) on ice for 15 min and further incubated with 1–2 ng of α-^{32}P-labeled doubled-stranded ARE-7 (the PPAR response element from the adipocyte fatty acid-binding protein gene) or AP-1 element (26) for an additional 30 min. The reaction mixture was then resolved on a 6% nondenaturing polyacrylamide gel in 4× TBE (45 mM Tris, 45 mM boric acid, 1 mM EDTA). The gel was dried and subjected to autoradiography. For a supershift analysis, polyclonal antibodies against c-Fos,

FosB, JunD, or PPARγ (Santa Cruz Biotechnology, Inc., Santa Cruz, CA) were added and incubated for an additional 20 min after the 30-min incubation.

Transient Transfection and Reporter Gene Assay—To determine whether PPARγ expressed by the adenoviral vector induces the PPAR response element (PPRE) promoter activity, HSC were transiently transfected with a PPRE-luciferase construct (tk-PPRE × 3-luciferase) using Targefect F-2 (Advanced Targeting Systems, San Diego, CA). To examine the effect of PPARγ expression on AP-1 activity, HSC transduced with Ad.PPARγ or Ad.GFP were transiently transfected with an AP-1 luciferase construct containing seven repeats of TGACTAA from the 12-*O*-tetradecanoylphorbol-13-acetate-responsive element (Stratagene, La Jolla, CA). We also examined the effects of CBP/p300 expression on the PPARγ-mediated effect on AP-1 by co-transfecting the Ad.GFP or Ad.PPARγ HSC line with a CBP/p300 expression plasmid (a kind gift from Dr. Stallcup, University of Southern California). For the determination of transfection efficiency, *Renilla* phRL-TK vector was used (Promega, Madison, WI). For transfection, 10-day cultures of HSC or HSC line in 6-well plates (70,000 cells/well; 3 days after infection with a viral vector) were incubated with 2 μg of each reporter construct, 0.02 μg of *Renilla* phRL-TK, and 2 μl of F-2 reagent in 1 ml of serum-free high glucose DMEM. Two h later, 1 ml of DMEM with 10% FBS was added to achieve the final FBS concentration of 5% for overnight incubation. On the next day, the medium was changed to DMEM with 10% FBS, and the cells were incubated for another 30 h. The cell lysate was collected for determination of both firefly and *Renilla* luciferase activities using the Dual-Luciferase reporter assay system (Promega). The results were normalized by *Renilla* luciferase activity.

Morphological Analysis—To investigate the effects of PPARγ on the HSC morphology, 7-day cultured HSC were transduced with Ad.GFP, Ad.PPARγ plus Ad.GFP, or Ad.PPARγ plus Ad.dn.PPARγ using a total MOI of 100 of virus and cultured for an additional 5 days. The cells were examined under a fluorescent microscopy and photographed for documentation. The cells were also fixed in 3% paraformaldehyde in a phosphate buffer for 1 h and washed with a phosphate buffer. Stress fibers were subsequently stained with rhodamine-labeled phalloidin for 30 min and washed with a phosphate buffer, and differential interference contrast images were acquired to assess the effects of PPARγ expression.

Retinyl Palmitate Measurement—To investigate the effect of PPARγ on the formation of intracellular lipid droplets, the cells were cultured with retinol (5 μM), palmitate (100 μM), or both for 48 h and stained with Oil Red O solution (in 60% isopropyl alcohol) for 20 min followed by counterstaining with hematoxylin. The stained slides were examined and photographed using an inverted light microscope. For chemical quantification of retinyl palmitate (a predominant vitamin A form stored in HSC), lipids were extracted with methanol and hexane from HSC treated with both retinol and palmitate (27). Retinyl palmitate in the hexane-extractable lipid phase was analyzed by reverse-phase high pressure liquid chromatography (HPLC) with the wavelength detector set at 325 nm. To prepare samples for HPLC analysis, solvent was evaporated from portions of lipid extracts in a 37 °C water bath using a gentle stream of N_2. Samples were resolubilized in 1:1 methanol-chloroform solvent before HPLC. For data acquisition and peak area integration, the Winflow software package system (Inus Systems, Tampa, FL) was used. The data were standardized with the cell number. The HPLC analyses were performed at the Cell Biology Core of the USC Research Center for Liver Diseases.

Western Blot Analysis of Cellular Proteins—HSC were cultured in a 100-mm dish for 7 days. On day 7, HSC were transduced with Ad.GFP or Ad.PPARγ using an MOI of 100 and cultured for additional 5 days. On day 12, cells were washed with PBS once and lysed with a lysis buffer (20 mM Tris-HCl, pH 7.6, 20 mM NaF, 20 β-glycerophosphate, 0.5 mM Na_3VO_4, 2.5 metabisulfite, 5 mM benzamidine, 1 mM EDTA, 0.5 mM EGTA, and 300 NaCl, with 10% glycerol and protease inhibitors and 1% Triton X-100). The lysates were stored at −80 °C until assayed. An equal amount of the whole cell protein (100 μg) was separated by SDS-PAGE and electroblotted to nitrocellulose filters. Proteins were detected by incubating the filter with monoclonal anti-α-smooth muscle actin (Sigma), rabbit polyclonal anti-type I collagen (Rockland Inc., Gilbertsville, PA), anti-PPARγ, or anti-JunD antibody (Santa Cruz Biotechnology) at a concentration of 0.2–2 μg/10 ml in TBS (100 mM Tris-HCl, 1.5 M NaCl, pH 7.4) with 5% nonfat milk followed by incubation with a horseradish peroxidase-conjugated secondary antibody (Santa Cruz Biotechnology) at 1 μg/10 ml. Proteins were detected by a chemiluminescent method using the PIERCE ECL kit (Amersham Biosciences).

JNK Assay—To assay the activity of JNK, HSC transduced with Ad.GFP or Ad.PPARγ were lysed for collection of the whole cell proteins as described above. Each 100 μg of lysate was used to immunoprecipitate with 2 μg of anti-JNK1 antibody (Santa Cruz Biotechnology). Immunoprecipitates were then incubated with 2 μg of the N-terminal peptide of c-Jun (Santa Cruz Biotechnology) in 30 μl of kinase reaction buffer (20 mM Tris-HCl, pH 7.5, 20 mM $MgCl_2$, 2 mM dithiothreitol) containing 20 μM ATP and [γ-^{32}P]ATP (0.5 μCi) for 1 h at 30 °C. The protein mixture was resolved by 10% SDS-PAGE followed by a transfer onto a nitrocellulose membrane and exposure of the membrane to a PhosphorImager. Phosphate incorporated into c-Jun was visualized. Total JNK levels were determined by immunoblot analysis.

PPARγ Immunoprecipitation and JunD Immunoblot Analysis—In order to assess the protein-protein interaction between PPARγ and JunD, *in vitro* translated PPARγ and JunD were incubated with an anti-PPARγ antibody (Santa Cruz Biotechnology) for 2 h. Protein A/G beads were added and incubated for another 24 h. Beads were washed three times and subjected to SDS-PAGE. Blots were probed with rabbit polyclonal anti-JunD antibody (2 μg/10 ml) in TBS containing 5% nonfat milk. Horseradish peroxidase-conjugated secondary antibody (1 μg/10 ml) was added and incubated followed by detection of JunD with the ECL reagent as described.

Glutathione S-Transferase (GST) Pull-down Assay—Expression vectors for GST, GST-PPARγ (pGEX-4T2 and pGEX-4T2-PPARγ provided by Dr. Akira Sugawara, Tohoku University School of Medicine, Sendai, Japan), and GST fusion proteins of PPARγ deletion mutants (pGEX-4T1-PPARγ deletion mutants provided by Dr. Shigeaki Kato, University of Tokyo, Tokyo, Japan) were produced in *Escherichia coli* BL21. The glutathione beads were coated with the fusion proteins by incubating both together overnight at 4 °C. JunD protein was translated *in vitro* from pcDNA3-mJunD plasmid (kindly provided by Dr. Sunita K. Agarwal, National Institutes of Health, Bethesda, MD) in the presence of [^{35}S]methionine using the TNT-T7-coupled reticulocyte lysate system (Promega, Madison, WI). The binding assay was conducted by incubating overnight at 4 °C the fusion protein-coated beads with 25 μl of the *in vitro* translation reaction in a 300-μl total volume of a NETN buffer (20 mM Tris, pH 8, 100 mM NaCl, 1 mM EDTA) containing 0.01% Nonidet P-40. Beads were washed four times with NETN (0.01%) and analyzed by SDS-PAGE and autoradiography.

Statistical Analysis—All numerical data were expressed as means ± S.D. The significance of the difference between two groups was assessed using a standard *t* test.

RESULTS

Forced Expression of PPARγ and PPRE Transactivation by Ad.PPARγ in Activated HSC—We first validated the forced expression of PPARγ in culture-activated HSC transduced with Ad.PPARγ by Western blot analysis. Ad.GFP-transduced HSC as a control had no detectable PPARγ (Fig. 1*A*), confirming the previous finding in our and other laboratories that activation of HSC results in depletion of this transcription factor (16). As expected, Ad.PPARγ infection indeed resulted in the expression of PPARγ in HSC (Fig. 1*A*). Further, the forced PPARγ expression increased PPRE promoter activity by 250-fold as determined by transfection of HSC with a PPRE-luciferase reporter gene containing three copies of the PPRE linked to the thymidine kinase promoter (Fig. 1*B*).

Morphological Changes Induced by PPARγ Expression—We examined whether the restoration of PPARγ expression affected the morphological features of activated HSC. Culture-activated HSC transduced with Ad.GFP exhibited a large, flattened polygonal shape, the typical cell morphology of culture-activated primary HSC (Fig. 2*A*). Infection with Ad.PPARγ resulted in retracted and reduced cytoplasm with the reappearance of dendritic processes resembling the more quiescent HSC phenotype (Fig. 2*B*). Using an MOI of 50, the expression of the wild-type PPARγ (Ad.PPARγ) reproduced the similar morphological changes (Fig. 2*C*), and this effect was completely blocked by the co-infection of the cells with an adenoviral vector expressing a dominant negative mutant of PPARγ (Ad.dn.PPARγ, MOI 50) (Fig. 2*D*). For the control, we used an MOI of 50 of Ad.GFP, maintaining the total viral MOI of 100. Further, we tested the effect of PPARγ expression on actin cytoskeleton. The stress fibers were labeled with rhodamine-phalloidin. Ad.GFP-transduced cells showed prominent actin

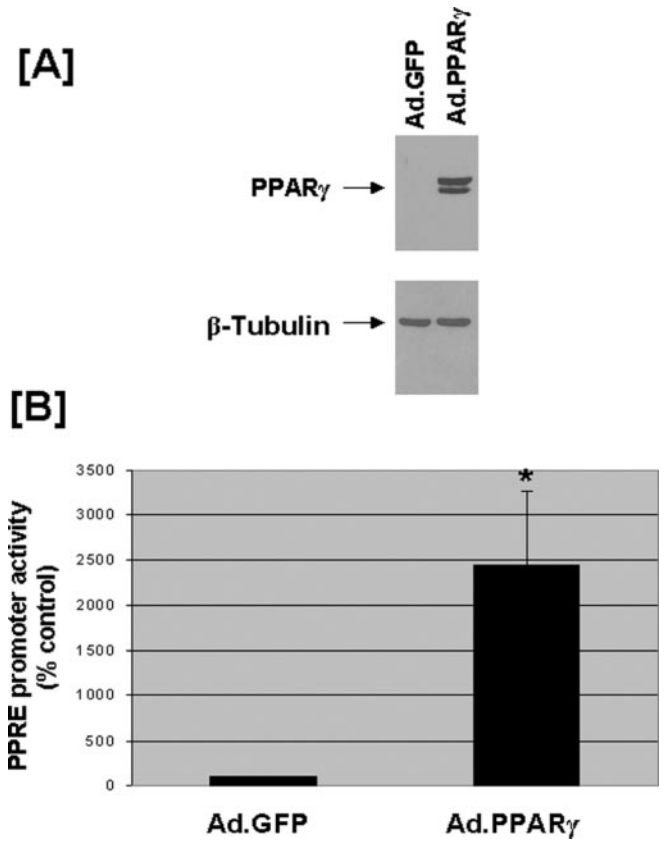

FIG. 1. **Adenovirus-mediated expression of PPARγ.** *A*, immunoblot analysis of nuclear proteins (25 μg each) from HSC transduced with Ad.GFP and Ad.PPARγ confirms the depletion of PPARγ in culture-activated former cells and sufficient expression of the transcription factor in the latter cells. Immunoblot for β-tubulin is shown as a control. *B*, PPARγ-driven PPRE promoter activity is conspicuously increased in Ad.PPARγ-transduced HSC as compared with Ad.GFP-transduced cells as shown by the transient transfection experiment with the PPRE-luciferase construct. *, $p < 0.05$ ($n = 6$) compared with the Ad.GFP-transduced cells.

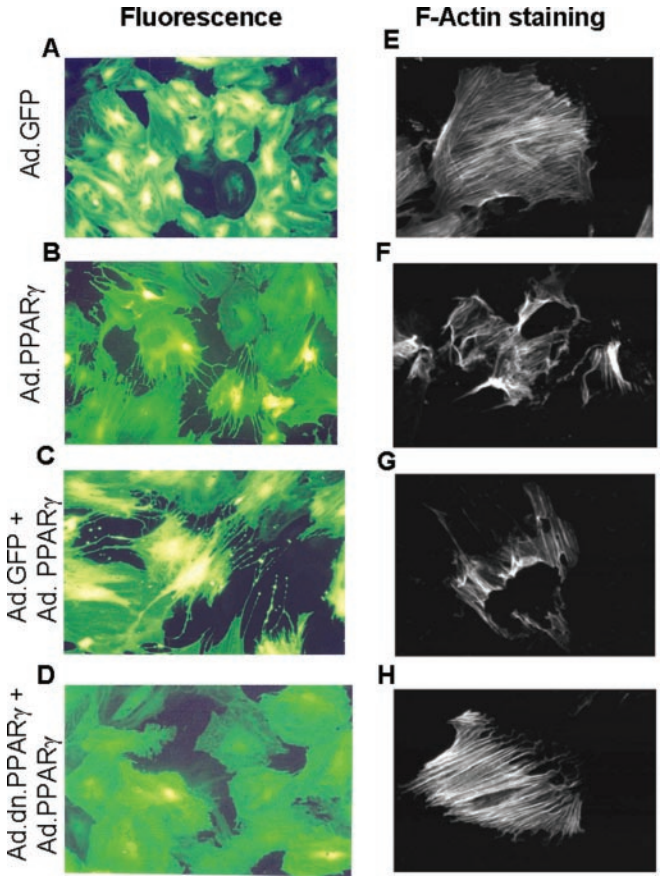

FIG. 2. **Forced expression of PPARγ causes the reversal of the activated morphology to the quiescent phenotype.** The morphology of the activated HSC is visualized by GFP fluorescence in culture-activated HSC transduced with the different adenoviral vectors, all expressing GFP (*A–D*). Ad.GFP-transduced cells show typical flattened, polygonal morphology of culture-activated HSC (*A*). PPARγ-expressing cells show retracted cytoplasm and the reappearance of dendritic processes, the morphologic features that resemble the quiescent HSC phenotype (*B*). Using 50 MOI each of Ad.PPARγ and Ad.GFP, a similar phenotype is attained (*C*), and this effect is abrogated by concomitant infection with Ad.dn.PPARγ (*D*). To examine the effect of PPARγ expression on actin cytoskeleton, stress fibers were labeled with rhodamine phalloidin. Ad.GFP-transduced, activated HSC showed prominent actin stress fibers (*E*) that are reduced in Ad.PPARγ-transduced HSC (*F*). This effect is also blocked by Ad.dn.PPARγ infection (*H versus G*).

stress fibers in a pattern typically observed in activated HSC (Fig. 2*E*). The cells expressing PPARγ showed an aberrant pattern of reduced stress fibers (Fig. 2*F*). This change in the stress fibers was also blocked by the co-infection with Ad.dn. PPARγ (Fig. 2*H*). In summary, these results demonstrate that the forced expression of PPARγ reverses the morphology of activated HSC to that of more quiescent HSC, and this effect is mediated by trans-activation of PPRE promoters as dn.PPARγ effectively abrogates the effect.

PPARγ Expression Decreases HSC Proliferation—One of the most obvious and important parameters of HSC activation is increased DNA synthesis. We have examined next whether the forced PPARγ expression inhibits this parameter. Forced expression of PPARγ in activated HSC caused a 70% inhibition in HSC DNA synthesis compared with that found in Ad.GFP-infected HSC controls (Fig. 3*A*).

PPARγ Expression Inhibits Expression of HSC Activation Marker Genes—To further validate the reversal of HSC activation at the functional level, we next examined the effects of PPARγ expression on mRNA expression of α1(I) procollagen and TGFβ1, the two *bona fide* activation markers expressed by HSC (28, 29). Real time PCR analysis revealed that α1(I) procollagen and TGFβ1 mRNA levels were significantly reduced by 60 and 40%, respectively, in Ad.PPARγ-transduced HSC as compared with Ad.GFP-transduced cells, whereas the PPARγ mRNA level showed an expected robust increase (Fig. 3*B*). We also performed immunoblot analyses for α-smooth muscle actin and type I collagen and demonstrated that the expression of both proteins were inhibited in Ad.PPARγ-transduced cells compared with Ad.GFP-transduced cells (Fig. 3*C*). Densitometric and statistical analyses of three sets of blots revealed that the expression of α-smooth muscle actin and type I collagen proteins in Ad.PPARγ-transduced cells was reduced to 31.7 + 28.3% ($p < 0.05$) and 30.0 + 15.7% ($p < 0.05$) of those in Ad.GFP-transduced cells, respectively. These results unequivocally confirm inhibition of myofibroblastic activation of HSC by forced PPARγ expression.

PPARγ Expression Allows HSC to Restore Their Ability to Accumulate Retinyl Esters—One of the characteristic functions of the quiescent HSC is the storage of vitamin A, which is significantly diminished in activated HSC (30). Thus, we examined whether the forced expression of PPARγ by Ad.PPARγ restored the ability of HSC to accumulate retinyl esters. For this, we have added retinol (5 μM), palmitate (100 μM), or both to the cultures of Ad.PPARγ- or Ad.GFP-transduced HSC. In Ad.GFP-transduced cells, the addition of retinol or/and palmitate did not significantly modify the lipid staining (Fig. 3*D*, *left panel*). Ad.PPARγ infection alone slightly increased the lipid staining regardless of whether they were treated with retinol

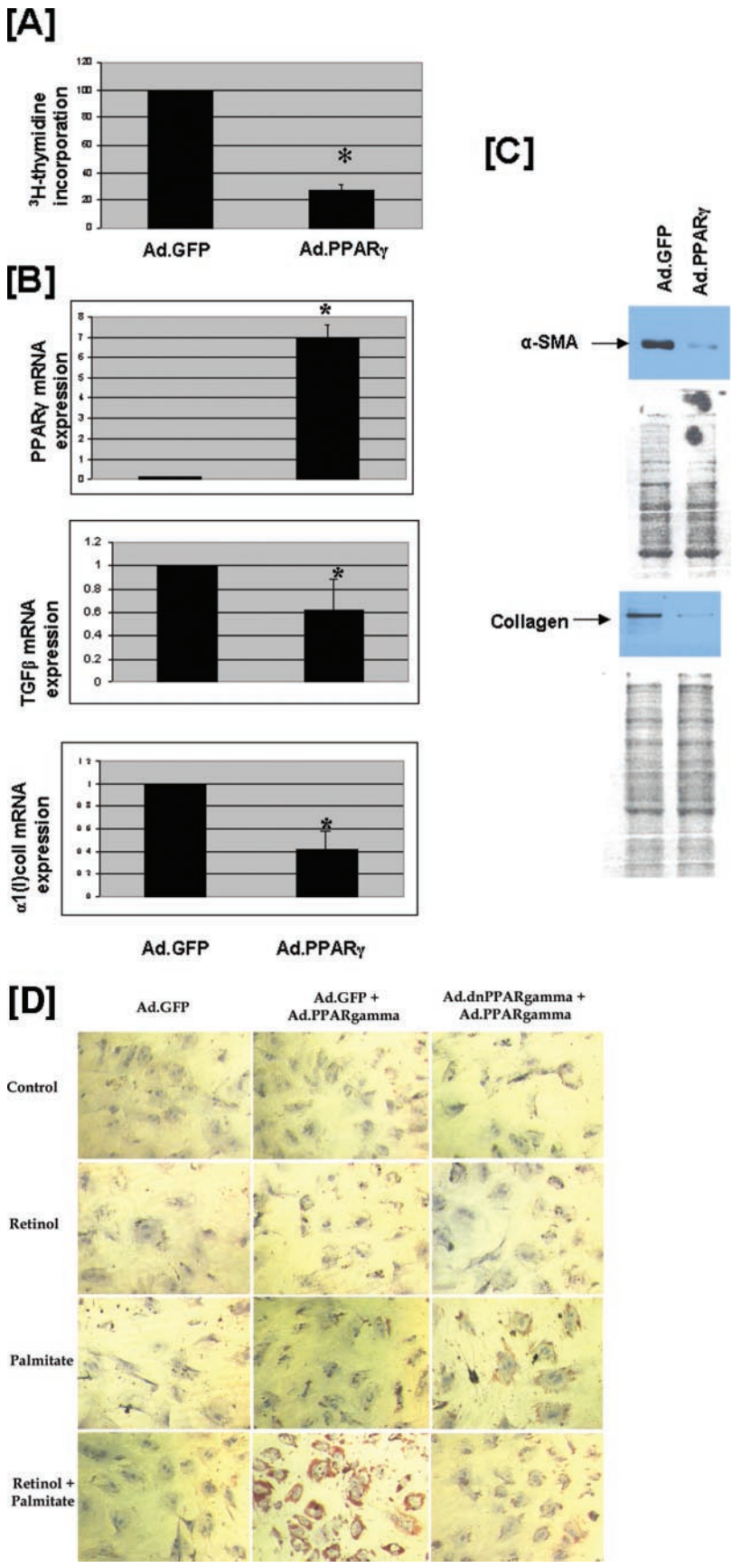

FIG. 3. **PPARγ inhibits activation markers and restores the capacity to accumulate retinyl esters.** *A*, Ad.PPARγ infection inhibits DNA synthesis as determined by incorporation of [^{3}H]thymidine. Note that PPARγ expression causes a 70% inhibition of DNA synthesis. *, $p < 0.05$ ($n = 3$). *B*, Ad.PPARγ infection causes an expected increase in PPARγ mRNA while inhibiting mRNA expression of α1(I) procollagen (−60%) and TGFβ1 (−40%) in culture-activated HSC as determined by Taqman PCR. *, $p < 0.05$ ($n = 3$). *C*, expression of α-smooth muscle actin (*α-SMA*) and type I collagen (*Collagen*) are inhibited in Ad.PPARγ-transduced HSC compared with Ad.GFP-transduced cells as assessed by immunoblot analysis. The equal protein loading is depicted by protein staining shown *below* each blot. *D*, accumulation of intracellular lipids is slightly increased by PPARγ expression (*Ad.PPARγ + Ad.GFP*) in the absence or presence of retinol or palmitate (*top three panels* of the *middle column*) as determined by staining with Oil Red O. Treatment of these cells with both retinol and palmitate results in marked accumulation of lipids, resembling quiescent HSC (*bottom*, *middle column*). These effects on intracellular lipids are partially blocked by the concomitant infection with Ad.dn.PPARγ (*right column*).

or palmitate alone (Fig. 3*D*, *middle panel*). However, the addition of both retinal and palmitate caused a conspicuous increase in the Oil Red O staining in these cells (Fig. 3*D*, *middle bottom panel*). The staining looked brownish in some cells due probably to microvesicular nature of lipid/retinoid storage in HSC. This type of lipid accumulation resembled the quiescent HSC cultured only for 1 day on plastic. The lipid accumulation caused by PPARγ was partially blocked by the expression of

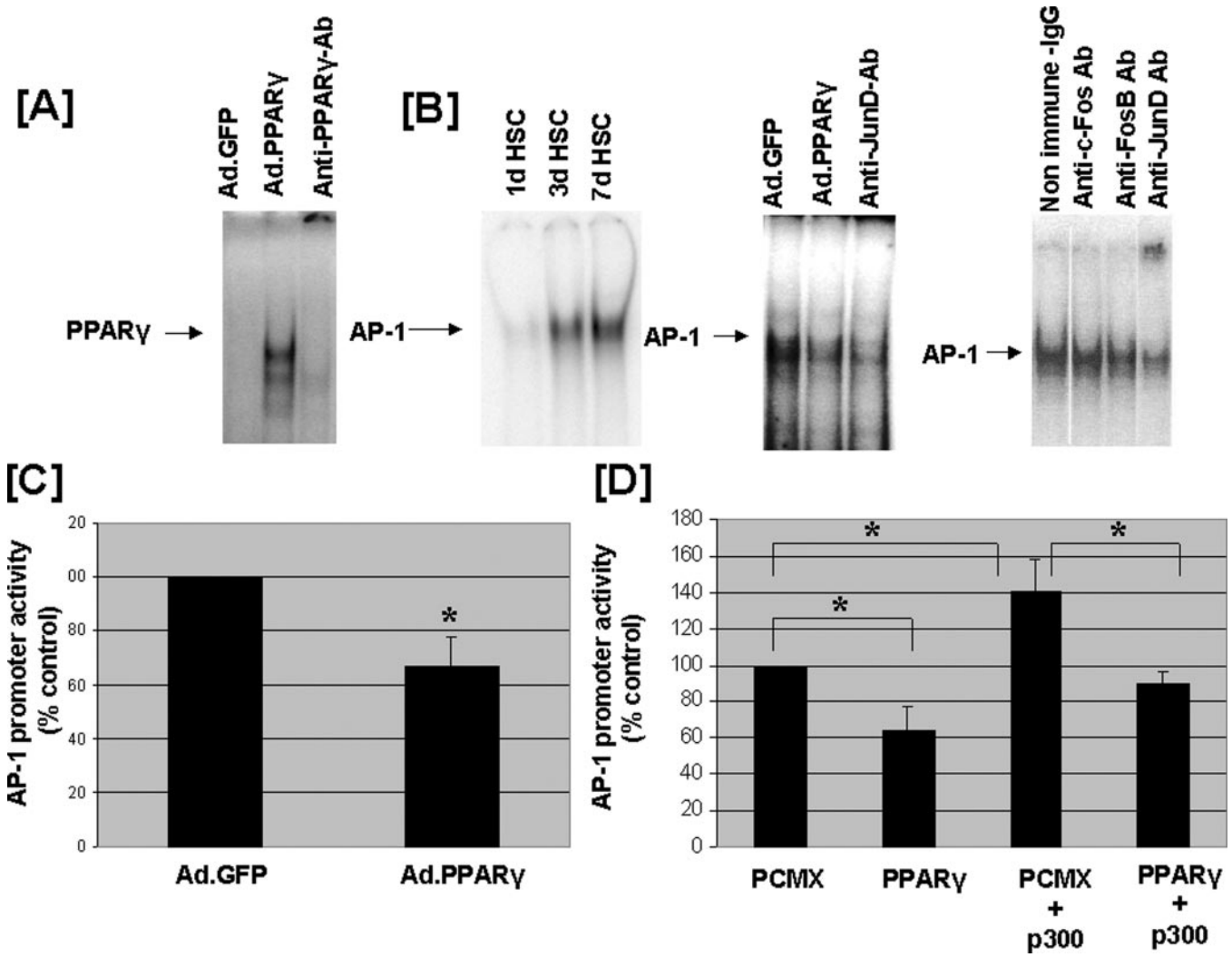

FIG. 4. **PPARγ expression inhibits JunD binding to AP-1 and AP-1 promoter activity.** *A*, PPARγ binding to the PPRE (ARE7) probe is increased in nuclear extracts prepared from HSC transduced with Ad.PPARγ as assessed by an electrophoretic mobility gel shift assay. Note that Ad.GFP-transduced cells have no appreciable binding, confirming the depletion of PPARγ in culture-activated HSC. The *last lane* shows supershift with anti-PPARγ antibody (*Ab*). *B*, in contrast to PPARγ binding, AP-1 binding is nearly absent in the quiescent HSC (1-day HSC) and increases as HSC become activated on day 3 and day 7 in culture (*first panel*). AP-1 binding is reduced in HSC transduced with Ad.PPARγ (*middle panel*). The *last lanes* of the *middle* and *right panels* show successful supershift of the AP-1 binding complex with anti-JunD antibody but not with anti-c-Fos or anti-FosB antibody (*second* and *third lanes* of the *right panel*). *C*, AP-1 promoter activity is decreased in Ad.PPARγ-transduced HSC line as demonstrated by transient transfection experiments using the AP-1 promoter luciferase construct. The data were standardized by the transfection efficiency as determined by *Renilla* luciferase activity. *, $p < 0.05$ ($n = 6$). *D*, overexpression of CBP/p300 does not prevent PPARγ-induced suppression of AP-1 promoter activity. The HSC line was co-transfected with a pCMX or PPARγ expression vector in the absence or presence of a p300 expression vector. Note that this experiment confirms the inhibition of AP-1 promoter activity by PPARγ (pCMX *versus* PPARγ). Overexpression of p300 increases AP-1 promoter activity in both pCMX- and PPARγ-transfected cells. However, the magnitude of PPARγ-mediated inhibition of AP-1 is not altered by p300 overexpression. *, $p < 0.05$ ($n = 3$).

dn.PPARγ (compare the *bottom panel* of the *middle* and *last* column). To validate that the accumulation of lipids really reflected increased storage of retinyl palmitate, the major species of stored retinyl esters in HSC *in vivo* (23), we analyzed the content of the retinyl ester in extracted lipids using reverse phase HPLC. Indeed, this analysis demonstrated a 3-fold increase in the content of retinyl palmitate in Ad.PPARγ-transduced HSC (9.0 ± 0.92 $\mu g/10^6$ cells) as compared with Ad.GFP-transduced cells ($2.9 + 1.23$ $\mu g/10^6$ cells) under the treatment of retinol and palmitate.

Reduced AP-1 Binding in PPARγ-expressing HSC—The results presented so far convincingly demonstrate that the forced expression of PPARγ in culture-activated HSC induces the reversal of the cell phenotype to that of quiescent HSC at both morphologic and biochemical levels. In order to investigate this effect at a more molecular level and to explore the mechanisms involved, we assessed the effects of the forced PPARγ expression on AP-1 binding, the parameter that is known to characterize and underlie many biochemical aspects of activated HSC (31). Nuclear extracts were prepared from Ad.GFP- and Ad.PPARγ-transduced HSC, and an electrophoretic mobility shift assay was performed. As a positive control, PPRE binding by PPARγ was assessed using an ARE-7 probe (a PPRE from the adipocyte fatty acid-binding protein gene), which more specifically binds PPARγ over PPARα (32). As shown in Fig. 4*A*, culture-activated HSC transduced with Ad.GFP were depleted of PPARγ binding to PPRE, which was significantly increased in PPARγ-expressing cells. The specificity of binding was supported by a supershift analysis using anti-PPARγ antibody (the *last lane* in Fig. 4*A*). Quiescent HSC (HSC cultured for 1 day) have minimal AP-1 binding activity, which is markedly increased on days 3 and 7 in culture (Fig. 4*B*). The robust AP-1 binding in activated HSC transduced with Ad.GFP was decreased significantly in the PPARγ-expressing cells (Fig. 4*B*).

The major components of AP-1 complexes in activated HSC were previously reported to be JunD, c-Fos, and FosB (33). A supershift analysis using antibodies against c-Fos, FosB, and JunD revealed that JunD was the main component of the AP-1 complex shown to bind to the DNA (Fig. 4*B*). Thus, these results demonstrate that PPARγ decreases JunD binding to the AP-1 site and suggest that this may be of potential significance in inhibiting DNA synthesis and expression of activation marker genes such as TGFβ1 and α1(I) procollagen.

PPARγ Expression Suppresses AP-1 Promoter Activity—Next, we examined whether the decreased AP-1 binding by PPARγ is associated with a decreased AP-1 promoter activity in Ad.PPARγ-transduced HSC. Transient transfection using an AP-1 promoter luciferase construct showed that the AP-1 promoter activity was indeed reduced by 40% in the HSC line transduced with Ad.PPARγ as compared with Ad.GFP-transduced cells (Fig. 4*C*).

Overexpression of p300 Co-activator Does Not Ameliorate PPARγ-mediated Inhibition of AP-1 Promoter Activity—Expression of one transcription factor may affect the activity of another trans-acting factor via a competition for a shared co-activator. In fact, p300 is a co-activator important for optimal transactivation of the promoter dependent on AP-1 (34) as well as that of the PPARγ-driven PPRE promoter (35, 36). Therefore, PPARγ-mediated inhibition of AP-1 activity may be a consequence of a competition for the limiting level of p300. To test this possibility, HSC cell line was transiently co-transfected with the AP-1 luciferase construct, a PPARγ expression vector or empty vector in the presence or absence of a p300 expression vector. In this experiment, we first confirmed that expression of PPARγ inhibited AP-1 promoter activity (Fig. 4*D*, *first two bars*). Expression of p300 increased AP-1 promoter activity regardless of whether PPARγ was co-expressed, indicating that p300 indeed serves as a co-activator for AP-1 (Fig. 4*D*, *last two bars*). However, the expression of p300 did not affect the magnitude of inhibition of AP-1 promoter caused by PPARγ (Fig. 4*D*). Therefore, the expression of p300 did not rescue the cells from the suppressive effect of PPARγ on AP-1 promoter activity, suggesting that p300 was not the limiting factor for AP-1 transcription in the presence of PPARγ.

Inhibited AP-1 Binding Is Not Due to a Change in JunD Expression or JNK Activity—To determine the mechanisms underlying inhibited AP-1 DNA binding in Ad.PPARγ-transduced HSC, we examined whether JunD mRNA or protein level was diminished in the cells. As shown in Fig. 5*A*, neither JunD mRNA nor JunD protein level was altered in Ad.PPARγ-transduced cells. Since JNK activity is required for phosphorylation of JunD for its activation, we tested next whether JNK activity was altered by forced PPARγ expression. JNK activity, as assessed by phosphorylation of GST-c-Jun, was not reduced in Ad.PPARγ-transduced HSC (Fig. 5*B*). Thus, these results suggest that expression and activation of JunD are not decreased by PPARγ expression in activated HSC.

The Direct Addition of PPARγ Dose-dependently Decreases JunD Binding to AP-1 Site—To test the possibility of direct inhibition of JunD binding by PPARγ, we tested whether *in vitro* translated PPARγ inhibited the binding of *in vitro* translated JunD to the AP-1 site. As depicted in Fig. 6*A*, the addition of PPARγ dose-dependently reduced JunD-mediated AP-1 binding. To confirm this effect using nuclear extracts from culture-activated HSC as an abundant source of JunD protein, an increasing amount of *in vitro* translated PPARγ was added to the extracts. This addition also decreased endogenous JunD binding in a dose-dependent fashion (Fig. 6*B*). These results suggested that PPARγ directly interacted with JunD to inhibit its binding to the AP-1 site.

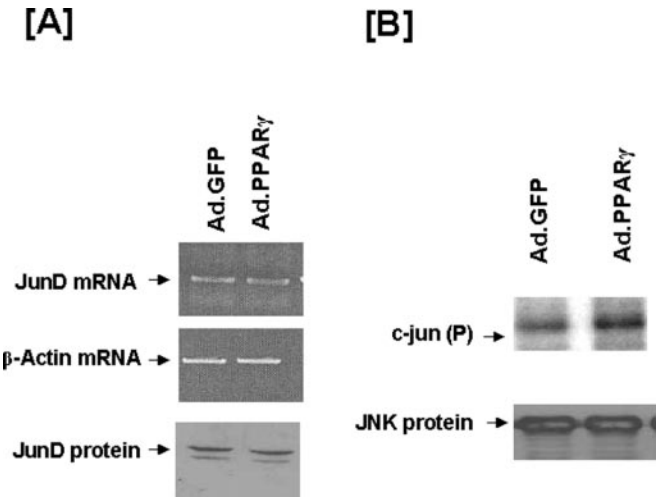

FIG. 5. **Neither JunD expression nor JNK activity is altered by PPARγ.** *A*, to examine the mechanisms of reduced AP-1 binding by PPARγ, the effects of PPARγ overexpression on JunD mRNA and protein levels in HSC were assessed by RT-PCR and immunoblot analyses. Note that PPARγ expression does not affect mRNA and protein levels of JunD. *B*, PPARγ expression also does not alter JNK activity and JNK protein levels as assessed by phosphorylation of GST-c-Fos and immunoblot analysis, respectively.

Neither PPARγ-selective Ligand nor RXRα Enhances the Inhibitory Effect of PPARγ on JunD Binding—Next, we determined whether the addition of a PPARγ-selective ligand (GW1929) potentiated the inhibitory effect of PPARγ on the binding of endogenous JunD to the AP-1 site. As shown in Fig. 6*C* (*lane 2 versus lane 4*), no additive effects of GW1929 were observed. These findings were also confirmed by an experiment using *in vitro* translated JunD (Fig. 6*D*, *lane 2 versus lane 4*). Since RXRα is a heterodimeric partner of PPARγ, we also assessed whether RXRα further decreased PPARγ-mediated JunD binding to the AP-1 site. Interestingly, RXRα alone decreased the binding of endogenous JunD (Fig. 6*C*, *lane 1 versus lane 5*) but not that of *in vitro* translated JunD (Fig. 6*D*, *lane 1 versus lane 5*) to the AP-1 site, suggesting the requirement of additional endogenous factor(s) for RXRα-mediated inhibition of AP-1 binding. However, the addition of RXRα together with PPARγ did not promote the inhibitory effect of PPARγ on JunD binding (Fig. 6, *C* and *D*, *lane 2 versus lane 6*).

PPARγ and a Dominant Negative Mutant of PPARγ (dn. PPARγ) Equally Inhibit AP-1 Binding—We next tested whether dn.PPARγ that blocked the morphologic effects of the wild type PPARγ could modify the inhibitory effect of PPARγ on AP-1 binding. Here adenoviral-mediated expression of PPARγ was again shown to inhibit AP-1 binding (data not shown). Interestingly, overexpression of dn.PPARγ alone also rendered the same inhibitory effect. Using 50 MOI each, the wild type PPARγ caused a moderate inhibition of AP-1 binding, and this was further suppressed by the addition of Ad.dn. PPARγ (data not shown). Both PPARγ and dn.PPARγ bound to the ARE7 probe with the same efficiency confirming the original finding that the mutations in the AF-2 region of PPARγ did not affect DNA binding but rather inhibited PPRE transactivation (25). These results demonstrate that dn.PPARγ equally inhibits AP-1 binding, and this inhibition does not appear to involve the AF-2 region.

PPARγ Physically Interacts with JunD—The direct interaction between PPARγ and JunD was suggested by the aforementioned results, and this notion was tested by co-immunoprecipitation and GST pull-down assays. For the former, *in vitro* translated PPARγ and JunD were incubated, PPARγ was immunoprecipitated with the specific antibody, and the precipi-

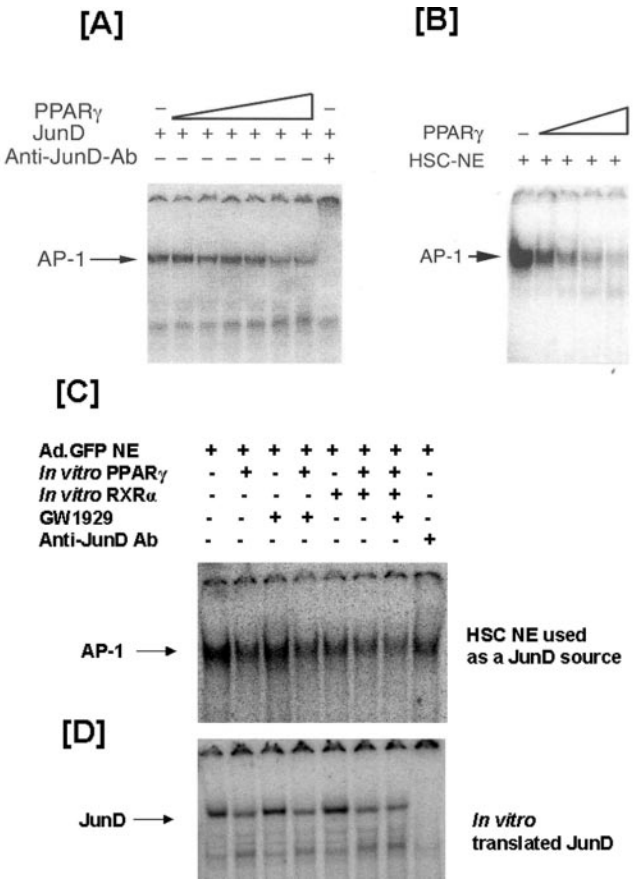

FIG. 6. The addition of increasing amounts of *in vitro* translated PPARγ dose-dependently decreases the binding of *in vitro* translated JunD (*A*) or endogenous JunD in HSC nuclear extracts (*NE*) (*B*) to the AP-1 probe as assessed by an electrophoretic mobility gel shift assay. The addition of *in vitro* translated RXRα or the PPARγ-specific ligand (GW1929) failed to promote the inhibition of the binding of endogenous JunD (C) or *in vitro* translated JunD (D) to the AP-1 probe. RXRα alone decreases the AP-1 binding by endogenous JunD (*lane 5* of *C*) but not that by *in vitro* translated JunD (*lane 5* of *D*).

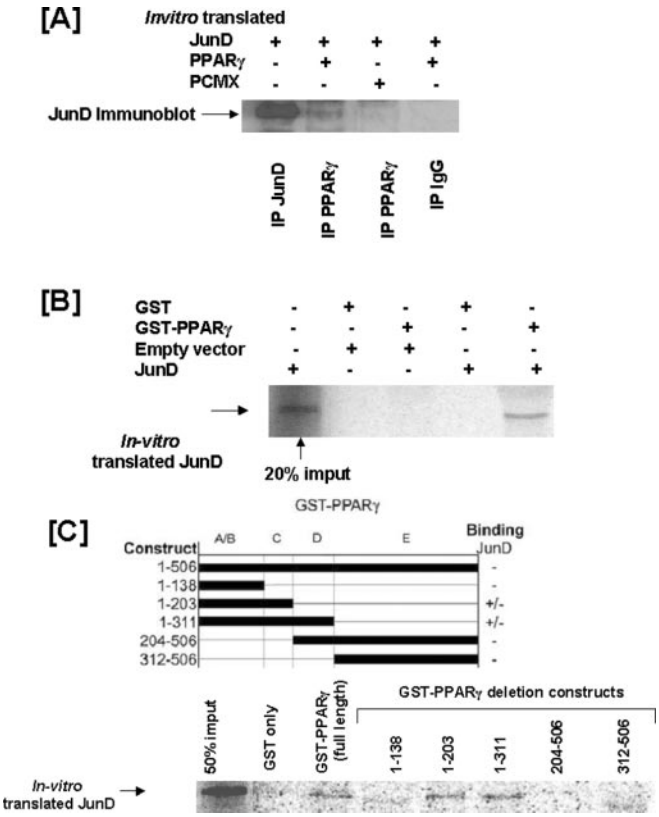

FIG. 7. **PPARγ interacts with JunD protein.** *A*, *in vitro* translated JunD and PPARγ were incubated together, and PPARγ was immunoprecipitated from the mixture. The precipitates were subjected to an immunoblot analysis for JunD. Note the presence of a JunD band in the *second lane*, whereas JunD immunoblots for the precipitate of the mixture containing no PPARγ (*PCMX*) and immunoprecipitation (*IP*) with nonimmune IgG showed no band. The *first lane* shows a positive control where *in vitro* translated JunD was immunoprecipitated with anti-JunD antibody followed by immunoblotting with the same antibody. *B*, for the GST pull-down assay, *in vitro* translated, ^{35}S-labeled JunD was detected when GST-PPARγ was pulled down with GSH beads from the incubation mixture of a JunD expression vector and the GST-PPARγ fusion protein (*lane 5*) but not from the mixture of the empty vector and the fusion protein (*lane 3*) or that of the JunD vector with no fusion protein (*lane 4*). *C*, full-length and five truncated GST-PPARγ fusion proteins were incubated with *in vitro* translated ^{35}S-labeled JunD. ^{35}S-Labeled JunD was detected when region 1–203 (*lane 5*) or region 1–311 (*lane 6*) but not region 1–138 (*lane 4*) was used. Further, the 204–506 region did not show any ^{35}S-labeled JunD (*lane 7*) band, suggesting that the region between 139 and 203 of PPARγ (C region; DNA binding region) is the primary region for the interaction with JunD.

tates were resolved on a gel and blotted with anti-JunD antibody. As shown in Fig. 7*A*, this procedure detected a band (*lane 2*) corresponding to the size of *in vitro* translated JunD (*lane 1*), whereas no expression of PPARγ (PCMX; *lane 3*) or immunoprecipitation with a nonimmune IgG (*lane 4*) failed to detect this band, suggesting a direct interaction between PPARγ and JunD. For the GST pull-down assay, *in vitro* translated, ^{35}S-labeled JunD was detected when GST-PPARγ was pulled down with GSH beads from the incubation mixture of a JunD expression vector and the GST-PPARγ fusion protein (Fig. 7*B*, *lane 5*) but not from the mixture of the empty vector and the fusion protein (*lane 3*) or that of the JunD vector with no fusion protein (*lane 4*). These results supported the notion that PPARγ and JunD indeed achieve a physical interaction, and this process interferes with JunD binding to the AP-1 element.

Assessment of the JunD-interacting Domain Using GST-PPARγ Deletion Mutants—To identify the domain of PPARγ that interacts with JunD, ^{35}S-labeled JunD was incubated with the following PPARγ deletion mutants: full-length, the A/B region only (residues 1–138); A/B and C regions (residues 1–203); A/B, C, and D regions (residues 1–311); D and E regions (residues 204–506); and E region only (residues 312–506). The pull-down results demonstrated that JunD interacted with the 1–203 or 1–311 mutant but not with the 1–138 mutant, suggesting that the C region (residues 139–203) is the primary domain for the interaction (*lanes 5* and *6*). The E region (residues 312–506) of PPARγ sometimes showed a much weaker interaction with JunD (data not shown).

DISCUSSION

The present study is the first to test whether forced expression of PPARγ, a nuclear receptor that is depleted in activated HSC, reversed the activated phenotype of the cells to the quiescent phenotype. Indeed, the adenovirus-mediated restoration of PPARγ resulted in the reappearance of morphologic features of quiescent HSC and inhibition of functional parameters for HSC activation such as increased DNA synthesis, the expression of α-smooth muscle actin, type I collagen, and TGFβ1. More importantly, the forced PPARγ expression restored the ability of the cells to accumulate retinyl palmitate, the unique and specific function of quiescent HSC *in vivo*. These results support our underlying hypothesis that PPARγ is required for the maintenance of the quiescent phenotype of HSC much like its requirement for adipocyte differentiation. This hypothesis was based on several lines of experimental evidence. Preadipo-

cytic fibroblasts can be differentiated into mature adipocytes when cultured in the condition that promotes induction of transcription factors that are essential for induction of adipocyte-specific genes. One such factor is PPARγ that is considered as a master regulator for adipogenesis (15). This adipogenic differentiation is inhibited by growth factors (platelet-derived growth factor and TGFα/epidermal growth factor) or cytokines (tumor necrosis factor α and leptin) that appear to impair the activities of PPARγ or other adipogenic transcription factors (37). Interestingly, these same soluble factors are also implicated in activation of HSC, and this activation is characterized by transdifferentiation of lipid-rich quiescent HSC to lipid-devoid myofibroblastic cells (38, 39). This analogy between adipocyte differentiation and HSC transdifferentiation is further supported by the fact that HSC express adipocyte- or preadipocyte-specific genes such as leptin (13). In fact, three laboratories including our own reported in 1999 that *in vitro* (16, 18) or *in vivo* (16, 17) activated HSC had reduced PPARγ levels and activities, and the treatment of activated HSC *in vitro* with the natural or synthetic ligands of PPARγ inhibited the diverse fibrogenic parameters of the cell activation (16). These studies were followed by an *in vivo* study by Galli *et al.* (17), who demonstrated effective prevention of the initiation of liver fibrosis and progression of preexisting liver fibrosis using toxic (dimethylnitrosamine or carbon tetrachloride) and cholestatic (bile duct ligation) animal liver fibrosis models and two PPARγ ligands (pioglitazone and rosiglitazone) (17). Thus, these findings collectively point toward the role of PPARγ as an anti-fibrogenic regulator in HSC that becomes depleted in activation of the cells. Indeed, the results presented in the current study definitively demonstrate the direct actions of PPARγ to reverse the activated phenotype without the use of exogenous ligands that are known to have receptor-independent effects as discussed in the Introduction (19–22). Further, our findings have far reaching implications beyond the therapeutic significance of PPARγ for liver fibrosis. They address the fundamental question of whether HSC transdifferentiation is analogous to adipocyte differentiation. Our previous analysis of the expression of PPARγ isoforms by an RNase protection assay demonstrated detection of the ubiquitous γ1 but not the adipocyte-specific γ2 isoform, indicating that HSC may not completely share the adipocyte phenotype (16). However, our present findings support a conclusion that similar regulatory mechanisms to those in adipocyte differentiation may exist in HSC transdifferentiation.

Another interesting finding from our study was that PPARγ facilitated both PPRE-dependent and -independent regulation of HSC. The morphologic reversal to the quiescent characteristics was dependent on PPRE promoter transactivation, since dn.PPARγ that exerts its effects at the promoter level blocked this morphologic effect. On the other hand, PPARγ-mediated inhibition of AP-1 promoter activity appeared to be at the level upstream of transcription and to be due to a direct interaction between PPARγ and JunD and consequent inhibition of JunD binding to the AP-1 site. There are numerous examples for this mode of negative cross-coupling between transcription factors. RAR and RXR are shown to inhibit AP-1 promoter activity via their ligand-dependent interactions with c-Jun (40) at their ligand binding domain. We also demonstrated inhibition of JunD binding to DNA by RXR when nuclear extracts but not *in vitro* translated JunD was used as the source of JunD. This differential effect is due probably to the presence or absence of an RXR ligand. In terms of PPARγ-mediated interactions, it is shown to physically interact with Smad3 to serve as a mechanism underlying ligand-mediated inhibition of expression of connective tissue growth factor in TGFβ-treated aortic smooth muscle cells (41). Further, PPARγ interacts with Sp1 and inhibits Sp1-mediated transcription of thromboxane receptor gene in vascular smooth muscle cells (42). PPARγ has most recently been shown to interact with NF-κB via PGC-2, an AF-1-specific co-activator for PPARγ. This complex formation inhibits PPARγ binding to DNA, and this mode of cross-coupling is suggested to play a role in shifting cellular differentiation of pluripotent mesenchymal stem cells to osteoblasts from adipocytes (43). They further showed that the DNA binding region of PPARγ was the interacting domain for p65. Our results with the deletion mutants also demonstrate that the same region was responsible for the interaction with JunD. However, in our study, *in vitro* translated PPARγ and JunD physically interacted without the presence of ligands or co-activators. Even when we used HSC nuclear extracts as the source of JunD, the inhibition of AP-1 binding by *in vitro* translated PPARγ was not promoted by the addition of the PPARγ-selective ligand or *in vitro* translated RXR, suggesting that the mechanisms of the protein-protein interaction in our experimental setting are different from previous studies and do not require either a heterodimer formation or activation of the complex with a ligand. Further, our finding that dn.PPARγ equally inhibited AP-1 binding suggests that this inhibition does not require AF-2-specific co-activators. Inhibition of JunD binding by PPARγ shown in our study has direct physiological implications in regulation of HSC activation, since JunD/AP-1 activity is shown to be important in expression of TGFβ (40), collagen (44), matrix metalloproteinase (8), tissue inhibitor of matrix metalloproteinase-1, and interleukin-6 (9) gene transcription. Indeed, suppressed JunD binding by adenovirus-mediated expression of PPARγ resulted in inhibition of both TGFβ and α1(I) procollagen gene expression in HSC (Fig. 3*B*).

The most striking phenotypic change facilitated by PPARγ was the restoration of the ability of HSC to accumulate retinyl palmitate when retinol and palmitate were presented to the cells. Since Ad.PPARγ infection alone or the concomitant addition of palmitate only slightly induced lipid accumulation, it appears unlikely that adipogenic differentiation was fully attained by these experimental conditions. Rather, these results suggest that PPARγ expression promoted the HSC-specific function of storing retinyl esters. It is interesting that this phenotype was partially blocked with dn.PPARγ, suggesting that induction of PPRE-driven genes may be partly involved. The understanding of the mechanisms underlying this effect requires further analysis of the genes involved in retinol esterification in HSC. Similarly, the morphologic reversal to the quiescent phenotype by PPARγ was dependent on the PPRE activity, suggesting the involvement of genes regulated by PPRE in attaining the morphologic effects. Further analysis of the genes involved in cytoskeletal organization and cell adhesion will be required to better understand the molecular mechanisms of the morphologic effects.

In summary, our results demonstrate that culture-activated HSC can be phenotypically and functionally reversed to the cells with the quiescent phenotype by forced expression of PPARγ. These results conceptually support the importance of PPARγ in the maintenance of the quiescent HSC phenotype. We also demonstrate a physical interaction of PPARγ with JunD but not alterations in JunD expression or JNK activity as part of the mechanisms underlying inhibition of JunD binding to DNA and AP-1 promoter activity. Our findings support the notion that PPARγ itself is the important effector molecule for controlling transdifferentiation of HSC. Whether and how other adipogenic transcriptional programs are involved in regulation of HSC are intriguing questions that need to be explored in the future.

Acknowledgments—We acknowledge invaluable assistance of Dr. Hal Yee Jr. and Andrew Melton in training Dr. Saswati Hazra for the staining technique for stress fibers, the service rendered by Dr. Murad Ookhtens and John Kulhlenkamp for HPLC analysis of retinyl palmitate, the training by Dr. Nori Kasahara for adenoviral vector amplification and purification, and technical training by Hongyun She during Dr. Saswati's graduate study.

REFERENCES

1. Hautekeete, M. L., and Geerts, A. (1997) *Virchows Arch.* **430,** 195–207
2. Kim, Y., Ratziu, V., Choi, S. G., Lalazar, A., Theiss, G., Dang, Q., Kim, S. J., and Friedman, S. L. (1998) *J. Biol. Chem.* **273,** 33750–33758
3. Kojima, S., Hayashi, S., Shimokado, K., Suzuki, Y., Shimada, J., Crippa, M. P., and Friedman, S. L. (2000) *Blood* **95,** 1309–1316
4. Buck, M., Kim, D. J., Houglum, K., Hassanein, T., and Chojkier, M. (2000) *Am. J. Physiol.* **278,** G321–G328
5. Lang, A., Schoonhoven, R., Tuvia, S., Brenner, D. A., and Rippe, R. A. (2000) *J. Hepatol.* **33,** 49–58
6. Hellerbrand, C., Jobin, C., Licato, L. L., Sartor, R. B., and Brenner, D. A. (1998) *Am. J. Physiol.* **275,** G269–G278
7. Knittel, T., Dinter, C., Kobold, D., Neubauer, K., Mehde, M., Eichhorst, S., and Ramadori, G. (1999) *Am. J. Pathol.* **154,** 153–167
8. Smart, D. E., Vincent, K. J., Arthur, M. J., Eickelberg, O., Castellazzi, M., Mann, J., and Mann, D. A. (2001) *J. Biol. Chem.* **276,** 24414–24421
9. Vincent, K. J., Jones, E., Arthur, M. J., Smart, D. E., Trim, J., Wright, M. C., and Mann, D. A. (2001) *Gut* **49,** 713–719
10. Neubauer, K., Knittel, T., Aurisch, S., Fellmer, P., and Ramadori, G. (1996) *J. Hepatol.* **24,** 719–730
11. Niki, T., Pekny, M., Hellemans, K., Bleser, P. D., Berg, K. V., Vaeyens, F., Quartier, E., Schuit, F., and Geerts, A. (1999) *Hepatology* **29,** 520–527
12. Cassiman, D., van Pelt, J., De Vos, R., Van Lommel, F., Desmet, V., Yap, S. H., and Roskams, T. (1999) *Am. J. Pathol.* **155,** 1831–1839
13. Potter, J. J., Womack, L., Mezey, E., and Anania, F. A. (1998) *Biochem. Biophys. Res. Commun.* **244,** 178–182
14. Yamada, M., Blaner, W. S., Soprano, D. R., Dixon, J. L., Kjeldbye, H. M., and Goodman, D. S. (1987) *Hepatology* **7,** 1224–1229
15. Spiegelman, B. M., and Flier, J. S. (1996) *Cell* **87,** 377–389
16. Miyahara, T., Schrum, L., Rippe, R., Xiong, S., Yee, H. F., Jr., Motomura, K., Anania, F. A., Willson, T. M., and Tsukamoto, H. (2000) *J. Biol. Chem.* **275,** 35715–35722
17. Galli, A., Crabb, D. W., Ceni, E., Salzano, R., Mello, T., Svegliati-Baroni, G., Ridolfi, F., Trozzi, L., Surrenti, C., and Casini, A. (2002) *Gastroenterology* **122,** 1924–1940
18. Marra, F., Efsen, E., Romanelli, R. G., Caligiuri, A., Pastacaldi, S., Batignani, G., Bonacchi, A., Caporale, R., Laffi, G., Pinzani, M., and Gentilini, P. (2000) *Gastroenterology* **119,** 466–478
19. Chawla, A., Barak, Y., Nagy, L., Liao, D., Tontonoz, P., and Evans, R. M. (2001) *Nat. Med.* **7,** 48–52
20. Straus, D. S., Pascual, G., Li, M., Welch, J. S., Ricote, M., Hsiang, C. H., Sengchanthalangsy, L. L., Ghosh, G., and Glass, C. K. (2000) *Proc. Natl. Acad. Sci. U. S. A.* **97,** 4844–4849
21. Baek, S. J., Wilson, L. C., Hsi, L. C., and Eling, T. E. (2003) *J. Biol. Chem.* **278,** 5845–5853
22. Lennon, A. M., Ramauge, M., Dessouroux, A., and Pierre, M. (2002) *J. Biol. Chem.* **277,** 29681–29685
23. Tsukamoto, H., Cheng, S., and Blaner, W. S. (1996) *Am. J. Physiol.* **270,** G581–G586
24. Xiong, S., Yavrom, S., Hazra, S., Wu, D., and She, H. (2001) *Hepatology* **34,** 520A (abstr.)
25. Gurnell, M., Wentworth, J. M., Agostini, M., Adams, M., Collingwood, T. N., Provenzano, C., Browne, P. O., Rajanayagam, O., Burris, T. P., Schwabe, J. W., Lazar, M. A., and Chatterjee, V. K. (2000) *J. Biol. Chem.* **275,** 5754–5759
26. Ohata, M., Lin, M., Satre, M., and Tsukamoto, H. (1997) *Am. J. Physiol.* **272,** G589–G596
27. Bhat, P. V., and Lacroix, A. (1983) *J. Chromatogr.* **272,** 269–278
28. Gressner, A. M., and Bachem, M. G. (1990) *Semin. Liver Dis.* **10,** 30–46
29. Bissell, D. M., Wang, S. S., Jarnagin, W. R., and Roll, F. J. (1995) *J. Clin. Invest.* **96,** 447–455
30. Friedman, S. L., Wei, S., and Blaner, W. S. (1993) *Am. J. Physiol.* **264,** G947–G952
31. Mann, D. A., and Smart, D. E. (2002) *Gut* **50,** 891–896
32. Juge-Aubry, C., Pernin, A., Favez, T., Burger, A. G., Wahli, W., Meier, C. A., and Desvergne, B. (1997) *J. Biol. Chem.* **272,** 25252–25259
33. Bahr, M. J., Vincent, K. J., Arthur, M. J., Fowler, A. V., Smart, D. E., Wright, M. C., Clark, I. M., Benyon, R. C., Iredale, J. P., and Mann, D. A. (1999) *Hepatology* **29,** 839–848
34. Janknecht, R., and Hunter, T. (1996) *Nature* **383,** 22–23
35. Mizukami, J., and Taniguchi, T. (1997) *Biochem. Biophys. Res. Commun.* **240,** 61–64
36. Gelman, L., Zhou, G., Fajas, L., Raspe, E., Fruchart, J. C., and Auwerx, J. (1999) *J. Biol. Chem.* **274,** 7681–7688
37. Gressner, A. M. (1996) *Kidney Int. Suppl.* **54,** S39–S45
38. Saxena, N. K., Ikeda, K., Rockey, D. C., Friedman, S. L., and Anania, F. A. (2002) *Hepatology* **35,** 762–771
39. Saile, B., Matthes, N., Knittel, T., and Ramadori, G. (1999) *Hepatology* **30,** 196–202
40. Salbert, G., Fanjul, A., Piedrafita, F. J., Lu, X. P., Kim, S. J., Tran, P., and Pfahl, M. (1993) *Mol. Endocrinol.* **7,** 1347–1356
41. Fu, M., Zhang, J., Zhu, X., Myles, D. E., Willson, T. M., Liu, X., and Chen, Y. E. (2001) *J. Biol. Chem.* **276,** 45888–45894
42. Sugawara, A., Uruno, A., Kudo, M., Ikeda, Y., Sato, K., Taniyama, Y., Ito, S., and Takeuchi, K. (2002) *J. Biol. Chem.* **277,** 9676–9683
43. Suzawa, M., Takada, I., Yanagisawa, J., Ohtake, F., Ogawa, S., Yamauchi, T., Kadowaki, T., Takeuchi, Y., Shibuya, H., Gotoh, Y., Matsumoto, K., and Kato, S. (2003) *Nat. Cell Biol.* **5,** 224–230
44. Chung, K. Y., Agarwal, A., Uitto, J., and Mauviel, A. (1996) *J. Biol. Chem.* **271,** 3272–3278